

MSSM radiative contributions to the $WW\gamma$ and WWZ form factors

A. Arhrib ^{a,b}, J.-L. Kneur ^{c*} and G. Moultaka ^a

March 26, 2022

^a Physique Mathématique et Théorique

Unité Associée au CNRS n° 040768,

Université Montpellier 2, F34095 Montpellier Cedex 5, France

^b Faculté des Sciences Semlalia, L.P.T.N.,

B.P. S15, Marrakesh, Morocco

^c CERN, Theory Division,

CH1211 Genève 23, Switzerland

Abstract

We evaluate one-loop contributions to the C and P conserving $WW\gamma$, WWZ form factors in the Minimal Supersymmetric Standard Model (MSSM), and in a more constrained Supergravity Grand Unified Theory (SUGRA-GUT). A systematic search of maximal effects in the available parameter space, shows that at LEP2 energy MSSM contributions can hardly reach the border of the most optimistic accuracy expected on those couplings, even for particles close to their production thresholds. At NLC energies, the effects are more comfortably of the order of the expected sensitivity, and may therefore provide useful information on MSSM parameter values which will not be available from direct particle production. We also discuss briefly some variance with other studies.

*On leave from U.R.A 768 du C.N.R.S., F34095 Montpellier Cedex France.

1. Introduction

The $WW\gamma$, WWZ Triple Gauge Couplings (TGC) will be directly measured with a decent accuracy of $O(0.1)$ or better at LEP2 [1] and, in a more remote future, with an accuracy of $O(10^{-3})$ at the Next Linear Collider (NLC) [2], i.e of the typical size of electroweak radiative corrections in the latter case. The effective Lagrangian parameterizing the most general trilinear WWV interaction obeying C and P symmetries is given by [3] [$V \equiv \gamma$ or Z]

$$\mathcal{L} = -ig_{VWW}[g_1^V V_\mu(W^{-\mu\nu}W_\nu^+ - W^{+\mu\nu}W_\nu^-) + \kappa_V V_{\mu\nu}W^{+\mu}W^{-\nu}] + \frac{\lambda_V}{M_W^2}V^{\mu\nu}W_\nu^{+\alpha}W_{\alpha\mu}^-] , \quad (1)$$

where $g_{\gamma WW} = e$, $g_{ZWW} = e \cot \theta_W$, and g_1^V , κ_V and λ_V are arbitrary, while the SM $SU(2)_L \times U(1)_Y$ gauge symmetry implies $g_1^\gamma = g_1^Z = 1$, $\kappa_\gamma = \kappa_Z = 1$, $\lambda_\gamma = \lambda_Z = 0$, at tree-level¹.

While such “anomalous” TGC are often purposed for parameterizing possible *tree-level* deviations from the non-abelian Standard Model (SM) gauge vertex, it is worth to emphasize that any renormalizable extension of the SM (and indeed the SM itself), gives non-trivial contributions to the TGC at the radiative correction level². But the generally expected decoupling [4, 5] of heavy new particles, plus the inherent appearance of typical $(4\pi)^{-2} \simeq 6 \cdot 10^{-3}$ from loops, lead to a largely consensual prejudice that such radiative effects may be generally small[6], in particular most likely below the reach of LEP2 measurements. However the fact that some of the supersymmetric partners could be relatively light give a complicated form factor dependence, threshold effects, etc..., which may substantially enhance the overall rough estimate above. Given the plausibility of the MSSM as a New Physics candidate, it is anyhow important to carry in some detail an exact evaluation of such virtual contributions, ascertaining eventually their irrelevance to LEP2 studies, and examining in quantitative terms their more likely relevance at NLC.

There have been in fact numerous evaluations of virtual contributions to TGC in the past, both in the SM [7, 8, 9, 10, 11] and supersymmetry[12, 13, 14, 15]. Most of these calculations were however carried within some approximation (e.g no Q^2 -dependence[7, 8, 12, 13], massless fermions[7], exact supersymmetry[12], etc). So far, the most complete analysis for the MSSM was performed in refs.[14] and [15]. In [14] the authors gave general analytic expressions for vertex contributions, but considered only the much more constrained SUGRA-GUT scenario in their numerical illustrations. Moreover, most of the previous analyses neglected the box contributions (apart from the ones which are crucial

¹ For $q^2 \neq 0$ (as it is in fact relevant here), the arbitrary coefficients in eq.(1) should be understood with a form-factor dependence, i.e $g_1^V(q^2)$, $\kappa_V(q^2)$ and $\lambda_V(q^2)$.

² Radiative corrections contribute to the C, P and CP violating TGC as well. We concentrate on C, P conserving contributions, since the sensitivity to the C, P violating (‘anapole’) coupling is expected to be less (by almost an order of magnitude)[1, 2], and the CP-violating TGC get radiative contributions only at the two-loop level in the SM or MSSM (provided that the soft susy terms are real).

to gauge-invariance issues, see section 3.2 below). An exception is ref. [15], where the *full* one-loop MSSM contributions to the $e^+e^- \rightarrow W^+W^-$ process were evaluated. Although these contributions implicitly contain TGC as a part, and give definite quantitative informations on the size of full MSSM corrections to that process, they are not expressed in terms of the parameters in eq.(1), which will be determined from the data in addition to the measurement of the $e^+e^- \rightarrow W^+W^-$ cross-section. It turns out to be difficult to extract from those results the parameters in (1) without redoing most of the calculation. The purpose of this letter is thus twofold: First we extend the work of Lahanas and Spanos (comparing by-the-way our results to theirs), by exploring in addition the unconstrained MSSM parameter space, in order to look for possible experimentally measurable effects at LEP2 and NLC. Secondly, we will illustrate with one partial but unambiguous (i.e gauge-invariant) representative case what TGC contributions can be expected from boxes. This raises in fact some general questions on the issues of both a gauge-invariant and unique definition of such TGC form factors.

2. Survey of relevant ingredients of the MSSM

As is well-known, the MSSM Lagrangian (restricted here to the R-parity conserving case) can be written as a supersymmetric part plus a (soft) supersymmetry breaking part, $\mathcal{L}_{MSSM} = \mathcal{L}_{susy} + \mathcal{L}_{soft}$. \mathcal{L}_{susy} involves the $SU(3) \times SU(2)_L \times U(1)_Y$ vector supermultiplets (gauge-bosons and their gaugino partners) and chiral supermultiplets (Higgs scalars and their Higgsino partners, leptons (quarks) and their slepton (squark) partners). The supersymmetry-breaking part \mathcal{L}_{soft} involves couplings among the scalars as well as the phenomenologically necessary splitting within each supermultiplet. For details we refer to [16, 17]. We simply list here the set of free MSSM parameters that we found convenient to choose in our subsequent analysis:

- $\tan \beta \equiv v_u/v_d$, the ratio of the two Higgs-doublet vacuum expectation values;
- the charged Higgs mass, M_{H^\pm} , which together with $\tan \beta$ determines (at tree-level) the CP-odd scalar mass M_A , the CP-even scalar masses $M_{h,H}$ and the mixing angle α defining physical scalar states (whereas the heavy top mass dominantly contributes to the radiative corrections which largely modify those tree-level mass values[18]);
- the H_d - H_u mixing parameter μ , appearing in the MSSM scalar potential (and entering also the gaugino mass matrices);
- the soft gaugino mass terms M_1, M_2^3 , which together with μ and $\tan \beta$ determine the chargino and neutralino mass eigenstates and couplings to the gauge bosons;
- finally all the soft squark and slepton mass terms, which due to the mixing between the left and right sfermions involve two mass eigenstates and a corresponding mixing angle: $\tilde{m}_1^i, \tilde{m}_2^i, \tilde{\theta}^i$ for any different squark and slepton flavor i .

³ note that the gluino mass term, M_3 , does not contribute to the TGC at the one-loop level

The unconstrained MSSM clearly gives a huge number of parameters to consider if no further theoretical assumptions are made. One attractive scenario is thus to consider the MSSM as emerging from a SUGRA-GUT[17]: in this case ⁴ one has, at the GUT scale, a universal scalar mass scale, $m_0(\Lambda_{GUT})$ for all sfermion mass terms; a universal gaugino mass, $M_1 = M_2 = M_3 = m_{1/2}(\Lambda_{GUT})$, and a unique trilinear soft term, $A_0(\Lambda_{GUT})$ (the latter only enters the sfermion mass mixing terms as far as TGC contributions are concerned). The various soft terms for any flavor at a chosen scale are then determined by the Renormalization Group (RG) running. An additional attractive feature is the possibility of radiative breaking of $SU(2)_L \times U(1)$ [17] within this scenario, which we will take into account when considering SUGRA-GUT contributions in our numerical illustrations ⁵. The remaining parameters accordingly are $\tan \beta$, the top mass (which we fix however to $m_{top} = 175$ GeV in the following), and the sign of μ . It would be of course interesting if SUGRA-GUT gave a distinct signature with respect to the unconstrained MSSM. In section 4. we illustrate the behavior of TGC as a function of the various MSSM or SUGRA-GUT parameters listed above.

3. Extracting TGC contributions from loops

In momentum space the vertex issued from the effective Lagrangian in (1) reads

$$\begin{aligned} \Gamma_{\mu\alpha\beta}^V = & ig_{VWW}\{f_V[2g_{\alpha\beta}\Delta_\mu + 4(g_{\alpha\mu}Q_\beta - g_{\beta\mu}Q_\alpha)] \\ & + 2\Delta\kappa'_V(g_{\alpha\mu}Q_\beta - g_{\beta\mu}Q_\alpha) + 4\frac{\Delta Q_V}{M_W^2}\Delta_\mu(Q_\alpha Q_\beta - g_{\alpha\beta}\frac{Q^2}{2})\}, \end{aligned} \quad (2)$$

where $2Q_\mu$, $(\Delta - Q)_\alpha$, and $-(\Delta + Q)_\beta$ designate the four-momenta and Lorentz indices of the *incoming* γ (or Z), W^+ , and W^- , respectively.

The coefficients in 2 are related to the original TGC parameters in (1) according to

$$\Delta\kappa'_V \equiv \kappa_V - 1 + \lambda_V = \Delta\kappa_V + \lambda_V; \quad \Delta Q_V \equiv -2\lambda_V. \quad (3)$$

Though trivial, the relations in (3) are important to remember when comparing the radiative contributions from a given model, generally more conveniently evaluated in terms of $\Delta\kappa'_V$, ΔQ_V [7]–[14], with the constraints obtained from simulated data, more traditionally given as bounds on $\Delta\kappa_V$ and λ_V . Note however that we disagree with [14, 9, 10] on an overall minus sign difference in (2) (thus in $\Delta\kappa_V$, λ_V). Our definitions in (2), (3) are consistent with SM tree-level couplings and, in particular, with the parametrization in [1]–[3] and [7].

⁴we disregard here the possibility of non-universal soft terms

⁵to determine the spectrum from RG running, we use for definiteness the procedure given in ref. [19]

3.1 Naive vertex contributions and gauge invariance

To extract from any triangle graph the contributions to $\Delta\kappa'_V$, ΔQ_V in eq.(2), we adopt a systematic procedure to deal with the large number of Feynman graphs contributing in the MSSM, avoiding as much as possible manipulation by hand. The relevant graphs are first evaluated analytically, using FeynArts and FeynCalc packages [20] including a full MSSM Feynman rules code [21]. Contributions to (2) are then systematically extracted by algebraic manipulation with the help of Mathematica[22]. We then can proceed to a purely numerical evaluation in terms of the standard Passarino-Veltman functions[23], with the help of FF-package [24]. We keep as well intermediate analytical expressions in terms of integrals over two Feynman parameters x, y , which turn out to be very compact and thus convenient to compare with similar analytical expressions previously obtained in the literature [7, 9, 14]. At this stage we obtain a complete agreement with the analytic results given in ref. [14] for the MSSM triangle graph contributions, apart from an overall minus sign as mentioned above. As noticed by these authors, the contributions from ordinary fermions differ however from previous results in the literature. In addition, several consistency cross-checks of our results were done, like e.g the vanishing of the total contributions to ΔQ_V for *exact* supersymmetry (for arbitrary Q^2), the decoupling behavior, $\Delta\kappa'_V, \lambda_V \rightarrow 0$ for large mass values (in the limit of MSSM parameters where it is expected to hold [5]), etc.

A problem which one immediately encounters is that the vertex graphs with virtual gauge bosons depend on the gauge fixing parameter, ξ in R- ξ gauges. These vertices need to be combined with parts of boxes and self-energies to become gauge-invariant. A general and non-ambiguous way of making such a gauge-invariant separation would be to fully project the on-shell amplitude on a complete operator basis (see for instance [25]), which would define by the same token the various WWV form factors (plus some remnant, non-TGC contributions [11]). Alternatively it was proposed to extract the desired gauge-invariant contributions directly, by so to speak ‘pinching’ the irrelevant propagator lines [26]. When applied to the TGC this allows to calculate only vertex-like, three-point functions, and was shown[10] to lead to a number of well-behaving features and properties expected from radiative corrections (simple Ward identities, good unitarity behavior, infra-red finiteness etc). Accordingly in our calculation we have included the pinch parts of box counterparts of the gauge-dependent vertices, and verified the aforementioned properties.

Now despite its simplicity and efficiency, the pinch technique raises some questions about the definition, universality, and extraction procedure of TGC quantities: by construction additional gauge invariant box contributions to TGC are left over. We shortly address this issue in section (5.) (a detailed treatment will be given elsewhere [27]).

4. TGC contributions in the MSSM

With the latter cautionary remarks in mind, we proceed to the numerical illustrations of the TGC from vertices plus the pinched box parts forming a gauge-invariant combination. We restrict here the study to $\Delta\kappa'_{\gamma,Z}$ and $\Delta Q_{\gamma,Z}$ among other anomalous couplings, since these (together with g_1^Z in eq. (1)) are expected to be measured with the best accuracy at LEP2 and NLC [2]. To illustrate the sensitivity to the various parameters in the unconstrained MSSM case, we give separately contributions from the Higgses (fig. 1), sfermions (fig. 2), and gauginos (fig. 3) ⁶, as functions of the parameters that we found the most illustrative in each case (see figure captions for details). A few additional comments may be useful:

In fig.1, the Higgses contribution becomes practically constant for $M_{H+} > 200$ GeV and/or $\tan\beta > 6-8$, approximately: for those values of $\tan\beta$, $M_h \rightarrow M_Z$ (+rad. corr.) and $M_H \simeq \text{const.} M_{H+}$, so there practically only remains the contribution from the approximately constant, light Higgs mass, m_h , while the other Higgses give decoupling contributions for large M_{H+} .

In fig.2, the sfermion contributions are shown. There are in principle so many arbitrary sfermion masses in the unconstrained MSSM that we have to make some choice in order to illustrate sfermion mass dependence. Accordingly, guided by the mass values obtained when searching for maximal effects (see the discussion below), we show here the variation of the *total* sfermion contributions versus one of the stop mass eigenvalues, \tilde{m}_{t1} , with other squark and slepton masses related to \tilde{m}_{t1} in a definite way (see figure caption for details). Of course we have tried many other configurations, and in particular since sfermion contributions can be either positive or negative, depending on the squark/slepton charges, one can obtain for the total sfermion contribution almost any possible value between the maximal and minimal ones, respectively given in table 1. As a general behavior however, we mention that the dependence upon the mixing angle is quite mild (with a maximum in magnitude for zero mixing); also the effects increase for increasing mass splitting between any up and down components (with positive effects dominated by the slepton contributions and negative effects dominated by squark contributions).

The gauginos contributions are illustrated in fig. 3 as function of the parameter μ , for some representative choice of the other relevant parameters ⁷ (see figure caption for details). The maximal effects in $|\Delta\kappa_{\gamma,Z}|$ are always due to chargino or neutralino threshold effects, and in some cases even anomalous threshold effects show up, as we checked explicitly (one example of the latter corresponds to the small discontinuities in $\Delta\kappa'_Z$ case b) of figure 3.B.). Note also that at LEP2 (Fig.3.A), $\Delta Q_{\gamma,Z}$ can become comparable to

⁶Note that those three different sources of TGC contributions do not mix at the one-loop level.

⁷Actually we should exclude on figure 3 a central band in μ corresponding to the present (LEP) and future (NLC) direct constraints on chargino/neutralino masses. We nevertheless kept the effects inside those bands for illustration.

$\Delta\kappa_{\gamma,Z}$ for large μ and away from threshold effects.

We have also performed a rather systematic search of maximal effects, with the help of standard minimisation tools [28]. Some typical 'large' effects are illustrated in table 1, both for separate sectors and total contributions. SM contributions are also given for comparison in table 1, for $m_{top} = 175$ GeV and $m_{Higgs} = 0.06 - 0.6$ TeV. One should note that the maximal effects in the MSSM are mostly (though not entirely) due to threshold effects, corresponding to the very unlikely case where most particle masses are very close to their direct production thresholds. For sfermion contributions however, as mentioned above large mass splittings between up and down components of a same doublet substantially increase the contributions. This can be understood by noting that no particular decoupling property is expected in that case: actually those contributions tend to a constant for very large mass splitting between up and down components. Furthermore, the extremal values illustrated in the figures, both for positive or negative contributions, are quite close to what we obtained from maximization. In table 1 we considered maximal effects only at $\sqrt{s} = 190$ GeV. At 500 GeV it is less compelling to look for maximal effects, given the trend of the contributions in this case. We simply quote here the (approximate) extremal values, in units of $(g^2/16\pi^2)$, for the *total* contributions obtained at this energy:

$$\Delta\kappa'_\gamma = -1.955; \quad \Delta\kappa'_Z = -0.99. \quad (4)$$

In all those illustrations we took into account as much as possible already existing constraints on some parameters, like the lightest Higgs mass, sfermions, and gauginos lower bounds, $\tan\beta$ constraints etc.

As a general remark, the magnitude of the effects tends to decrease at 500 GeV, with respect to LEP2 energies: this is indeed expected, once thresholds are crossed, in accord with the good unitarity behavior expected from a renormalizable gauge theory. Fortunately the expected accuracy of TGC measurements greatly increases at NLC [2], which more than compensates the latter effect.

In addition, we show in fig. 4 the *total* contributions for one particular SUGRA-GUT choice of parameters, the no-scale scenario [29], which was chosen to illustrate one constrained example in contrast with the general cases above. We have compared our results with the ones from [14] for different SUGRA-GUT parameter choices. Apart from the already mentioned overall sign difference everywhere, we have some discrepancies, namely for $\Delta\kappa'_\gamma$ and ΔQ_Z , which are very pronounced at high energy (500 GeV). On the other hand we get very good agreement (given the completely different numerical tools used, and, more essentially, the slightly different way of evolving the SUGRA-GUT parameters from Λ_{GUT} to low energy scales) with their results for $\Delta\kappa'_Z$ and ΔQ_γ . Accordingly, as far as we can see, the discrepancies cannot be traced to the slightly different way of evolving the parameters with the renormalisation group in our analysis. Our results show a more

rapid decoupling behavior at high energy, though that does not by itself guarantee correctness.

In summary, one can hardly expect to see any MSSM TGC at LEP2, where even the most optimistic accuracy expected, $|\Delta\kappa_\gamma| < 0.02 \simeq 6\text{--}7 (g^2/16\pi^2)$ [1], hardly compares with the maximal effects⁸ in table 1. In contrast the effects at NLC can be comfortably above the expected accuracy for a reasonably large range of the parameter space (taking $|\Delta\kappa_{\gamma,Z}| < 10^{-3} \simeq 0.3 (g^2/(16\pi^2)[2])$ as a reference accuracy at 500 GeV,). In particular, even for the more constrained SUGRA-GUT scenario we obtain effects above the accuracy limit, although the no-scale case illustrated in Fig.4 does not give the largest possible contribution. Accordingly, at a 500 GeV NLC it should even be possible to obtain useful information on the MSSM parameter space in the range which will not be accessible from direct production processes.

5. Additional non-pinch box contributions

The previous picture is valid if the genuine (i.e non-pinch) box contributions, generally omitted in most evaluation of TGC, are truly negligible. As mentioned in section 2 above, by construction the pinching takes from a box just what is necessary to cancel the ξ -dependence of vertices, therefore leaving out other possible gauge-invariant (box) contributions. The resulting combinations of pinch boxes plus vertices give a TGC contribution with s -dependence *only* [10], which in that sense is meant to be “process- independent” and universal. However it was noted earlier in SM [11], that once projecting the $e^+e^- \rightarrow W^+W^-$ one-loop corrections over the *complete* operator basis, the obtained TGC clearly exhibit both s and t dependence. One thing is that, to our knowledge, there is no proof that *no other* possible universal contributions from boxes are left out by the pinch technique. Even if the latter statement could be proven, one problem would persist, since experimentally there are a priori no planned procedure to distinguish ‘universal’ from ‘non-universal’ TGC. So far all analysis have extracted expected TGC constraints, from fitting angular distributions for simulated data to theoretical expressions assuming *t-independent* TGC⁹. Therefore, an unambiguous procedure to test a *specific model* prediction via TGC measurements, is to evaluate the full contributions to the definite process where TGC are extracted. This is of course a much more involved program,

⁸There are larger radiative corrections to the $e^+e^- \rightarrow W^+W^-$ process, especially at high energies, which are essentially due to QED Initial State Radiations (ISR) [25, 30]. Though those would formally contribute to the $g_1^{\gamma,Z}$ TGC in eq. (1) [11], they should obviously not be taken into account in our evaluation of New Physics virtual effects. In principle, those large ISR effects can be corrected for before extracting TGC from data.

⁹To distinguish a t -dependence, one would need typically to allow in the fit the TGC to be different for different scattering angles, which would most likely considerably reduce the expected accuracy on such TGC.

but to illustrate here simply what one should expect in general, we have evaluated one first partial but unambiguous (gauge-invariant) contribution, the sum of boxes with one internal chargino (resp. neutralino), two internal sneutrinos (resp. selectrons) and one internal selectron (resp. sneutrino), which do contribute to $\Delta\kappa'_\gamma$ and $\Delta\kappa'_Z$ yet cannot be obtained from the pinch technique. The results are shown on fig. 5 at $\sqrt{s} = 500$ GeV. The effects are clearly comparable to the vertex contributions, even when most of the chargino/neutralino masses are above threshold. In contrast, this particular box contribution is totally negligible at LEP2, giving at most $\mathcal{O}(0.1g^2/16\pi^2) \simeq 2.7 \cdot 10^{-4}$ TGC at $\sqrt{s} = 190\text{GeV}$. Of course this is only a partial contribution, so that no general conclusion can be drawn from it. What may be interesting on that particular example is that the t -dependence is relatively smooth, so that neglecting t -dependence in the fits may not introduce too much biases. In any case, even if such issue is irrelevant for LEP2, given the too small size of vertex contributions anyway, this example should emphasize the need to evaluate all other boxes at NLC energies: there, any source of TGC contribution is likely to be sizeable and, accordingly, one should be careful to sum all the relevant contributions if one wants a precise comparison to the data. The complete evaluation of boxes, together with a more detailed illustration of both MSSM and SUGRA-GUT contributions, is at present under investigation [27].

Acknowledgments

A. A. and G. M. acknowledge partial support from a EC contract CHRX-CT94-0579. J.-L. K. acknowledges support from a CERN fellowship. We are thankful to M. Carena, F. Jegerlehner, J. Papavassiliou, F. M. Renard and C. Wagner for useful discussions. We also thank A. Lahanas and V. Spanos for useful exchange of information.

References

- [1] M. Davier et al, Proceedings of the ECFA Workshop on LEP200, eds. A. Böhm and W. Hoogland, CERN Report 87-08 (1987) vol. 1 p.120; M. Bilenky, J.-L. Kneur, F.M. Renard and D. Schildknecht, Nucl. Phys. B 409 (1993) 22; R.L. Sekulin, Phys. Lett. B 338 (1994) 369; *Physics at LEP2*, “Triple Gauge Coupling” chapter, CERN 1995 Workshop report to appear, edited by G. Altarelli, T. Sjöstrand and F. Zwirner.
- [2] G. Gounaris et al, *e^+e^- Collisions at 500 GeV: the Physics potential*, ed. P. Zerwas, DESY 92-123B, p.735; T. Barklow, in *Proceedings of the Workshop on Physics with Linear Colliders*, Saariselka, Finland (1992) p.423; M. Bilenky, J.-L. Kneur, F.M. Renard and D. Schildknecht, Nucl. Phys. B 419 (1994) 240; M. Gintner, S. Godfrey and G. Couture, Phys.Rev. D52 (1995) 6249; V. Andreev, A. Pankov and N. Paver, preprint IC/95/293 (September 95).

- [3] K. Gaemers and G. Gounaris, Z. Phys. C1 (1979) 259; K. Hagiwara, K. Hikasa, R. Peccei and D. Zeppenfeld, Nucl. Phys. B 282 (1987) 253.
- [4] T. Appelquist and J. Carazzone, Phys. Rev. D11 (1975) 2856.
- [5] J.F.Gunion and T.Turski, Phys.Rev. D40 (1989) 2325.
- [6] C. Arzt, M. B. Einhorn and J. Wudka, Nucl. Phys. B433 (1995) 41.
- [7] W. A. Bardeen, R. Gastmans and B. Lautrup, Nucl. Phys. B46 (1972) 319.
- [8] G. Couture and J. N. Ng, Z.Phys. C35 (1987) 65
- [9] E. Argyres, G. Katsilieris, A. Lahanas, C.G Papadopoulos and V. Spanos, Nucl. Phys. B391 (1993) 23.
- [10] J. Papavassiliou and K. Philippides, Phys. Rev. D48 (1993) 4255.
- [11] J. Fleischer, J.-L. Kneur, K. Kolodziej, M. Kuroda and D. Schildknecht, Nucl. Phys. B378 (1992) 443, (E): *ibid.* B426 (1994) 246.
- [12] C. Bilchak, R. Gastmans and A. van Proyen, Nucl. Phys. B273 (1986) 46.
- [13] G. Couture, J.N. Ng, J.L. Hewett and T.G. Rizzo Phys. Rev. D38 (1988) 860.
- [14] A. B. Lahanas and V. C. Spanos, Phys. Lett. B334 (1994)378; hep-ph/9504340; E. Argyres, A. Lahanas, C.G Papadopoulos and V. Spanos, preprint UA/NPPS-18B (October 95).
- [15] S. Alam, Phys. Rev. D50 (1994) 124; *ibid.* 148; *ibid.* 174.
- [16] for a review of MSSM, see e.g. H.P. Nilles Phys.Rep. 110 (1984) 1; H. E. Haber and G. L. Kane, Phys. Rep. 117 (1985) 75.
- [17] for a recent review on SUGRA-GUT, see e.g R. Arnowitt and P. Nath, *Supersymmetry and Supergravity: Phenomenology and Grand Unification*, Brazil Summer School (1993):3-63 (e-print archive hep-ph/9309277) and earlier references therein.
- [18] Y. Okada, M. Yamaguchi and T. Yanagida, Prog. Theor. Phys. 85 (1991) 1; H. E. Haber and R. Hempfling, Phys. Rev. Lett. 66(1991) 1815; J. Ellis, G. Ridolfi and F. Zwirner, Phys. Lett. B257(1991) 83.
- [19] V. Barger, M. S. Berger and P. Ohmann, Phys. Rev. D49(1994) 4908.
- [20] J. Küblbeck, M. Bohm, A. Denner, Comput. Phys. Commun. 60 (1990) 165; R. Mertig, M. Bohm, A. Denner, Comput. Phys. Commun. 64 (1991) 345; H. Eck and S. Küblbeck, *Guide to FeynArts* 1.0 (Würzburg Univ. 1992); R. Mertig, *Guide to FeynCalc*, ed. 1.0 (Würzburg Univ. 1992).

- [21] A. Arhrib, Ph.D. Thesis, Université Montpellier II 1994 (unpublished)
- [22] S. Wolfram, *Mathematica*, Addison-Weisley (1988)
- [23] G. Passarino and M. Veltman, Nucl. Phys. B160(1979) 151.
- [24] G.J. van Oldenborgh, Comput. Phys. Commun. 66 (1991) 1.
- [25] W. Beenakker, F. Berends, M. Bohm, A. Denner, H. Kuijf and T. Sack, Nucl. Phys. B304(1988) 463;
J. Fleischer, F. Jegerlehner and M. Zralek, Z. Phys. C42 (1989) 409.
- [26] J. M Cornwall and J. Papavassiliou, Phys. Rev. D40 (1989) 3474, and references therein.
- [27] A. Arhrib, J.-L. Kneur and G. Moultaka, in preparation
- [28] F. James and M. Roos, *MINUIT, Function minimization and error analysis*, version 92.1 CERN 1992.
- [29] for a review of the no-scale Supergravity models, see A. B. Lahanas and D. V. Nanopoulos, Phys. Rep. 145(1987) 1.
- [30] W. Beenakker and A. Denner, Int. J. Mod. Phys. A9(1994) 4837.

Table Caption

Table 1: Maximal contributions to $\Delta\kappa'_V$ and $\Delta\kappa_V(\equiv \Delta\kappa'_V + \Delta Q_V/2)$ in unconstrained MSSM, at 190 GeV (*in units of $(g^2/16\pi^2)$*). The corresponding values of input parameters are indicated (all masses are in GeV). \tilde{U} and \tilde{D} denote generically all up and down squarks respectively. The SM (total) contributions are also shown for two values of M_h .

Figure Captions:

Fig.1.A: Total MSSM Higgs contribution at $\sqrt{s} = 190\text{GeV}$ to $\Delta\kappa'_{\gamma,Z}$ versus M_{H^+} for different values of $\tan\beta$. In all the plots the ordinate numbers are in units of $g^2/16\pi^2$;

Fig.1.B: same as for Fig. 1.A at $\sqrt{s} = 500\text{GeV}$

Fig.2.A: Total squark and slepton contribution to $\Delta\kappa'_\gamma$ and $\Delta\kappa'_Z$ versus $m_{\tilde{t}_1}$, at $\sqrt{s} = 190\text{GeV}$ with the following mass spectrum configuration : $m_{\tilde{t}_1} = m_{\tilde{t}_2} = m_{\tilde{U}_1} = m_{\tilde{U}_2} = m_{\tilde{l}_1} = m_{\tilde{l}_2}$ and $m_{\tilde{t}_1} + m_{\tilde{\nu}_L} \simeq m_{\tilde{t}_1} + m_{\tilde{D}_{1,2}} = 1.09\text{TeV}$;all left-right mixing angles are vanishing;

Fig.2.B: same as in Fig. 2.A at $\sqrt{s} = 500\text{GeV}$ except that now $m_{\tilde{t}_1} + m_{\tilde{\nu}_L} = 1.245\text{TeV}$ and $m_{\tilde{t}_1} + m_{\tilde{D}_{1,2}} = 1.47\text{TeV}$.

Fig.3.A: Total chargino/neutralino contribution to $\Delta\kappa'_{\gamma,Z}$ and $\Delta Q_{\gamma,Z}$ versus μ , at $\sqrt{s} = 190\text{GeV}$ with $M = 100\text{ GeV}$, $M' = 60\text{ GeV}$, $\tan(\beta) = 2$

Fig.3.B: Total chargino/neutralino contribution to $\Delta\kappa'_\gamma$ and $\Delta\kappa'_Z$ versus μ , at $\sqrt{s} = 500\text{GeV}$, case a) $M = 190\text{GeV}$, $M' = 70\text{GeV}$, $\tan(\beta) = 2$, case b) $M = 350\text{GeV}$, $M' = 175\text{GeV}$, $\tan(\beta) = 2$;

Fig.4.A: $\Delta\kappa'_\gamma$ and $\Delta\kappa'_Z$ at $\sqrt{s} = 190\text{GeV}$, in no-scale SUGRA-GUT ($m_0 = A_0 = 0$) as a function of $m_{1/2}$. Both $\mu < 0$ and $\mu > 0$ cases are illustrated;

Fig.4.B: Same as in Fig.4.A for $\sqrt{s} = 500\text{GeV}$;

Fig.5: An example of non-pinch box contributions to $\Delta\kappa'_\gamma$ and $\Delta\kappa'_Z$, the sum of boxes with one internal chargino (resp. neutralino), two internal sneutrinos (resp. selectrons) and one internal selectron (resp. sneutrino) versus the W^- production angle θ , (defined with respect to the beam axis) in $e^+e^- \rightarrow W^+W^-$, with $m_{\tilde{e}_1} = m_{\tilde{\nu}_L} = 260\text{GeV}$, zero left-right mixing angle; case a) $M = \mu = 150\text{GeV}$, $M' = 100\text{GeV}$, $\tan(\beta) = 15$; case b) $M = M' = \mu = 250\text{GeV}$, $\tan(\beta) = 2$.

Contribution ($\sqrt{s} = 190$ GeV)	$\Delta\kappa'_\gamma$	$\Delta\kappa_\gamma$	$\Delta\kappa'_Z$	$\Delta\kappa_Z$
W, Z, γ +fermions ($m_t=175$)	2.59	2.338	1.37	1.13
Higgses ($\tan\beta = 1.5, M_{H^+} = 95$)	0.369	0.344	0.457	0.427
sfermions	3.730	2.919	1.561	1.133
($m_{\tilde{e}_{1,2}} = m_{\tilde{\mu}_{1,2}} = m_{\tilde{\tau}_1}$ $= m_{\tilde{U}_1} \simeq 92$; $m_{\tilde{D}_1} = m_{\tilde{\nu}} \simeq 45$);				
gauginos	0.750	0.889	0.304	0.429
($M \simeq 73, M' \simeq 10, \mu \simeq -88$)				
Total MSSM	7.439	6.490	3.692	3.119
SM ($m_t=175, M_h=65-600$)	1.800–2.291	1.530–2.039	1.499–1.406	1.231–1.166

Table 1

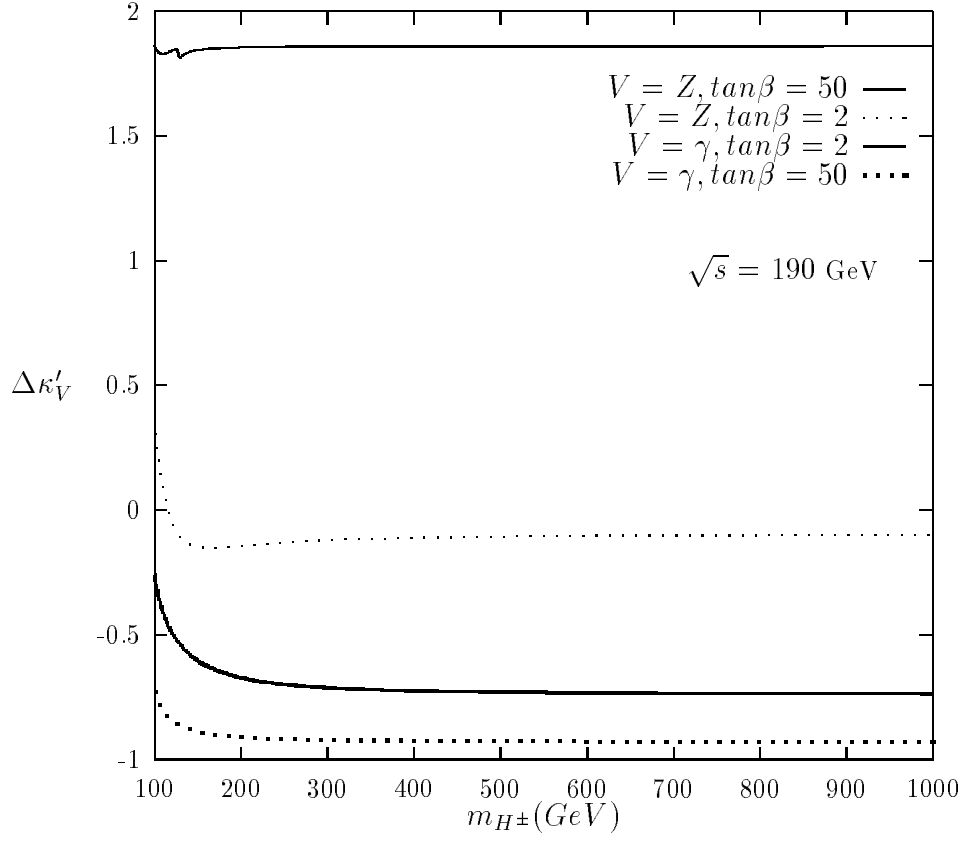
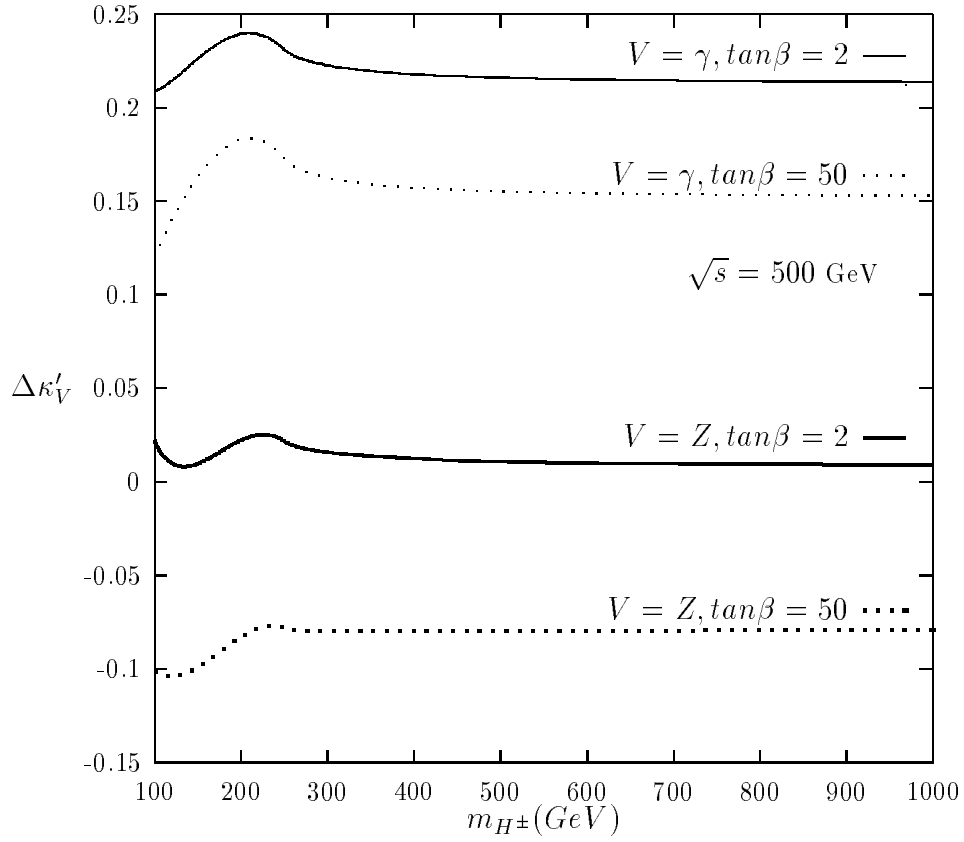
Fig.1.A**Fig.1.B**

Fig.2.A

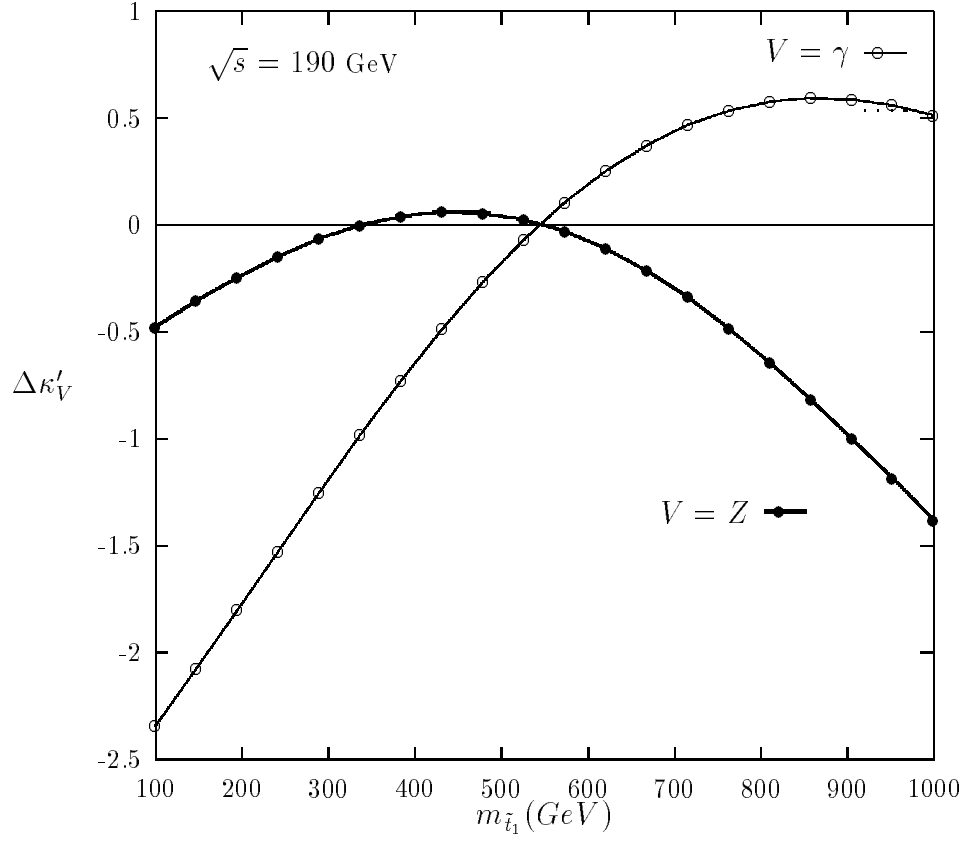


Fig.2.B

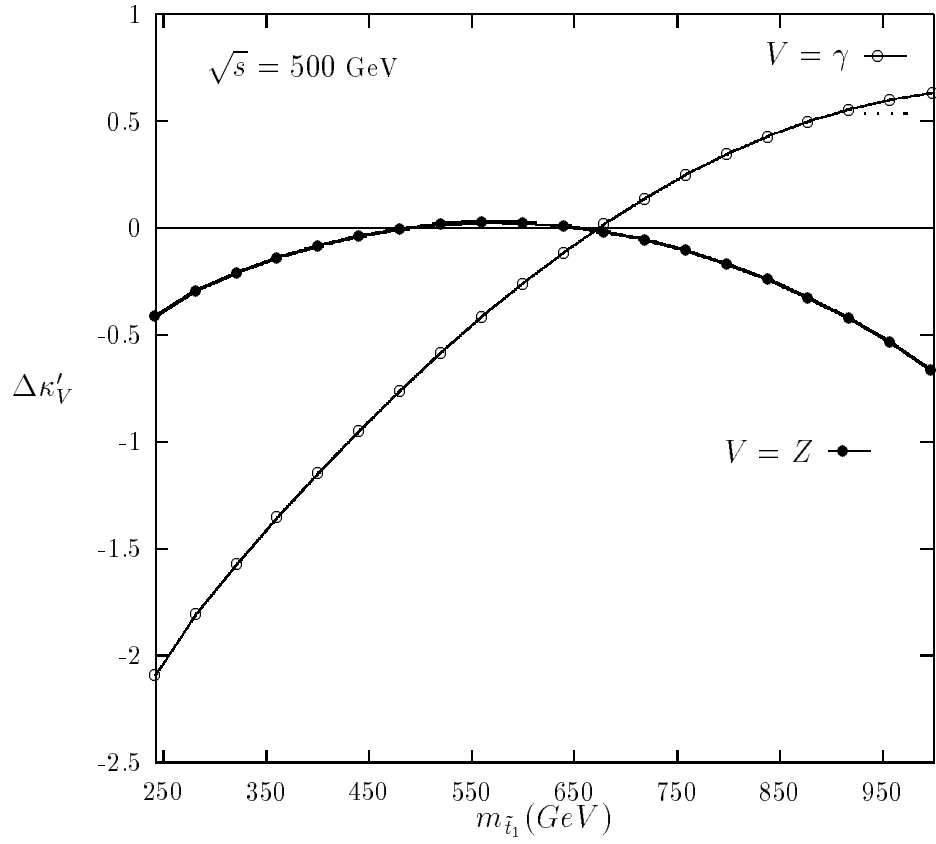


Fig.3.A

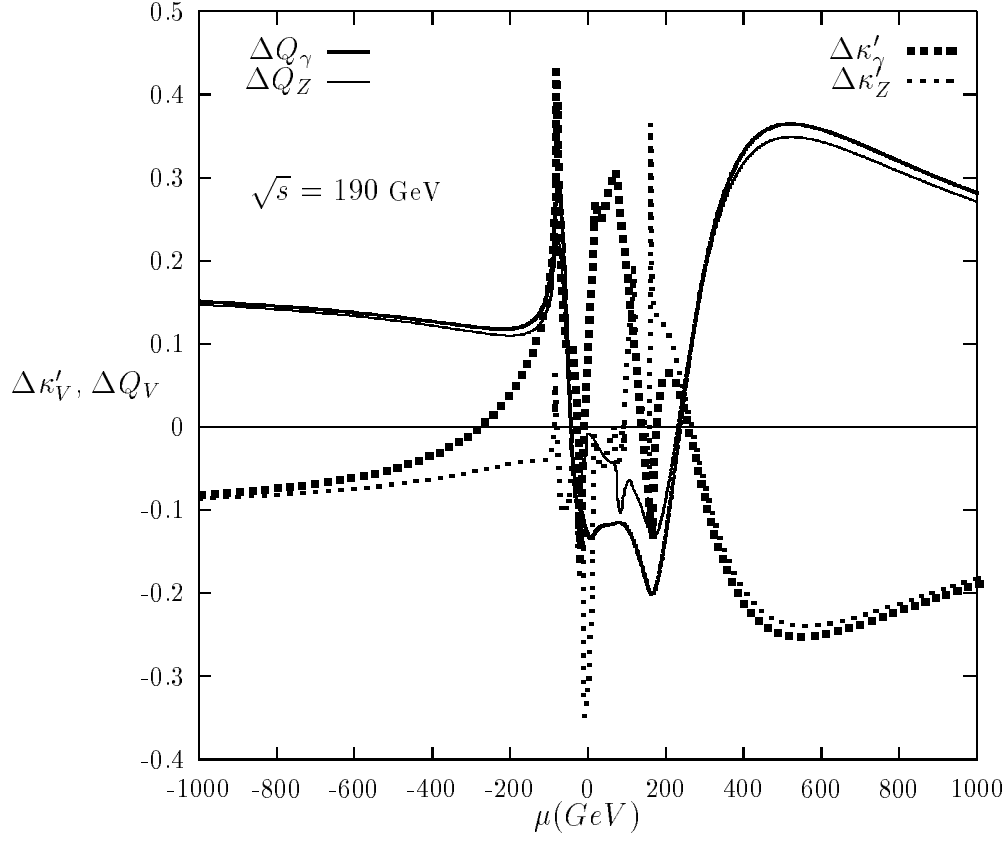


Fig.3.B

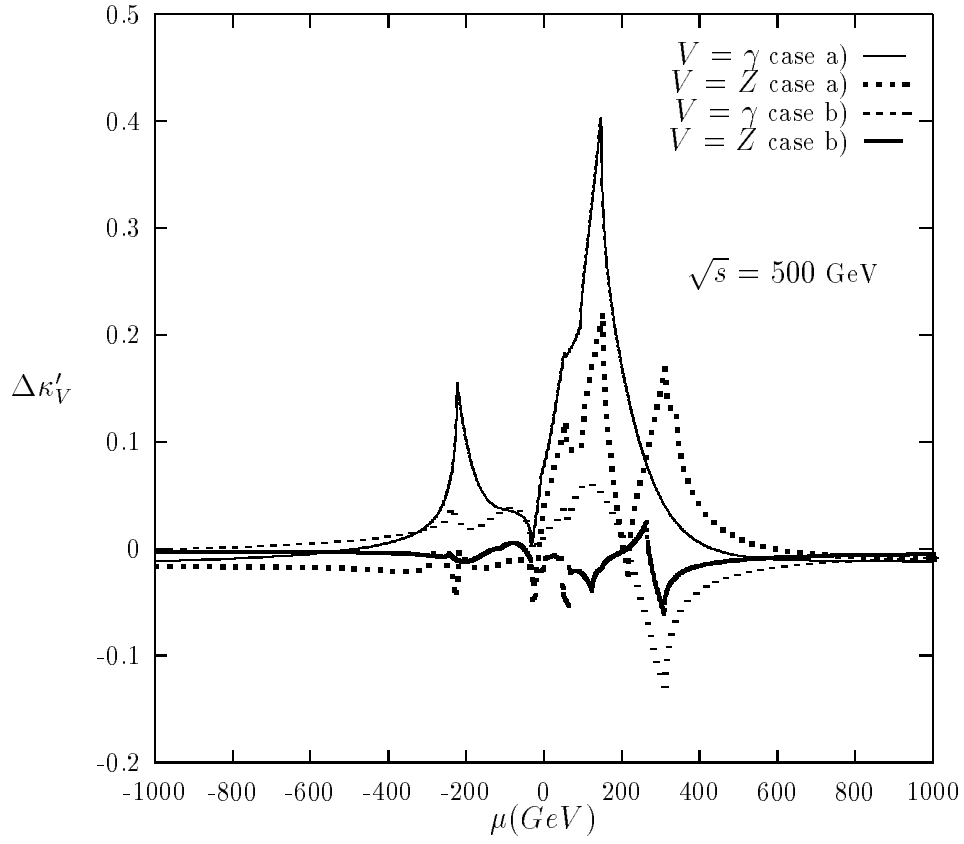


Fig.4.A

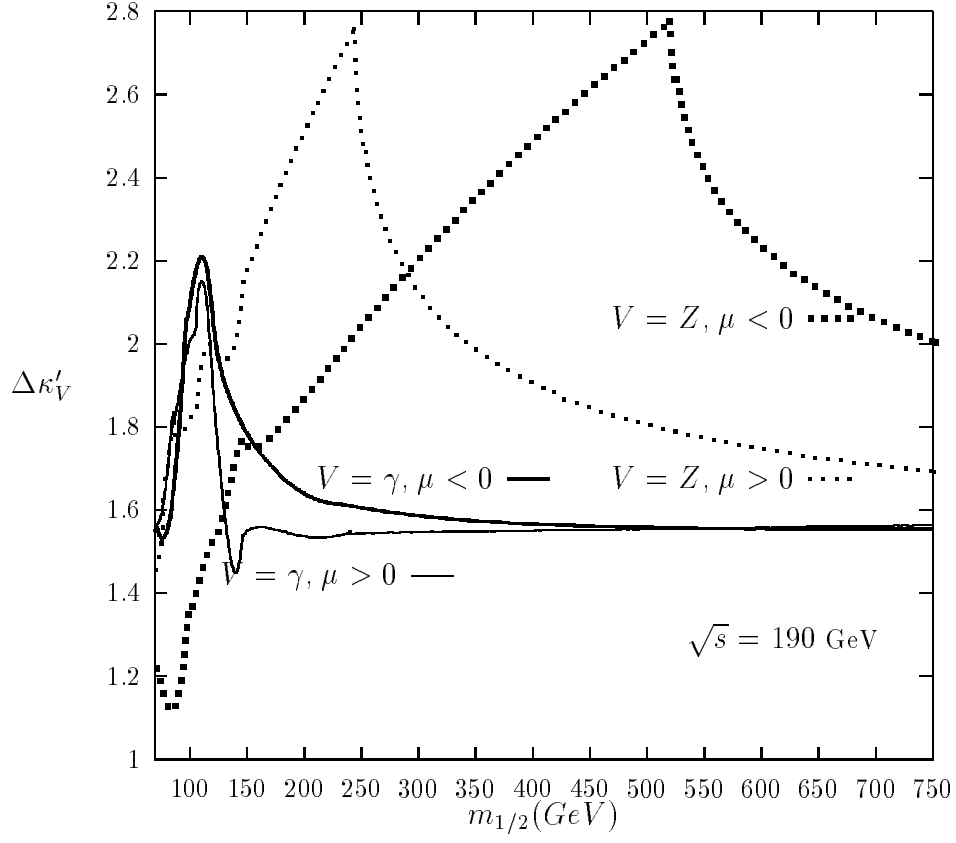


Fig.4.B

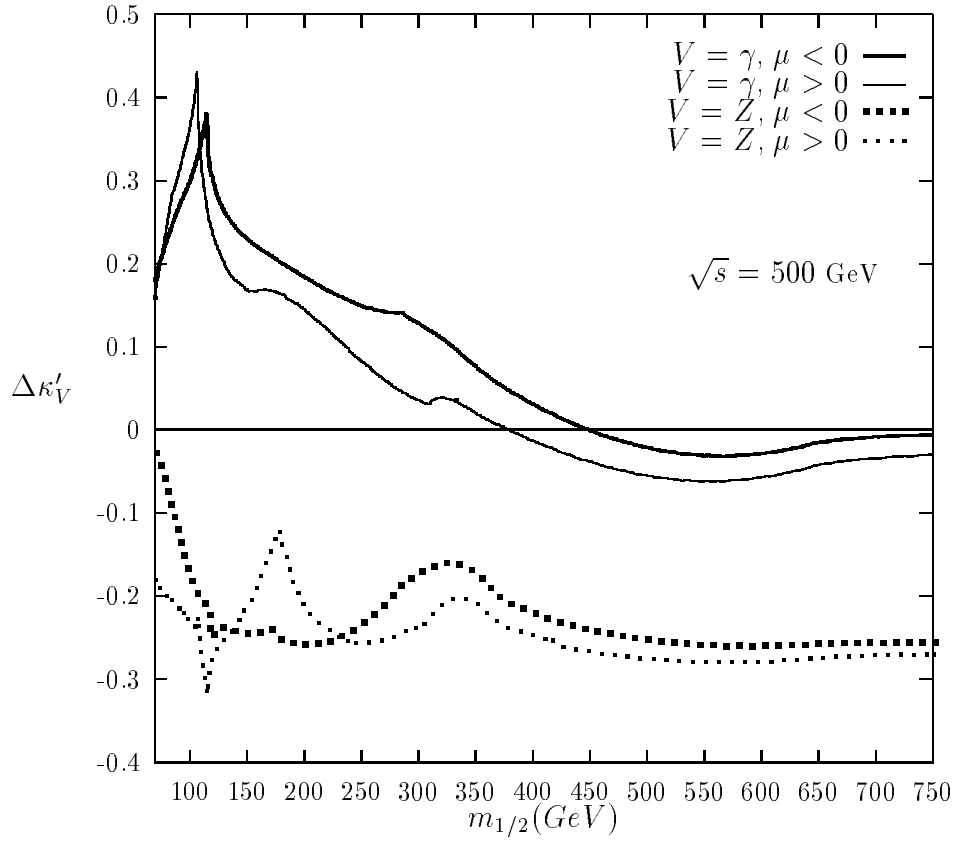


Fig.5